THE BULLETIN OF OKAYAMA UNIVERSITY OF SCIENCE No. 53 A pp. 1-10(2017)

Giant resonance in electronic stopping power of carbon for MeV-per-atom C60 fullerene ions

Toshiaki KANEKO
Department of Applied Physics,
Faculty of Science,
Graduate School of Science,
Okayama University of Science,
1-1 Ridai-cho, Kita-ku, Okayama, 700-0005, Japan

(Received October 31, 2017; accepted December 4, 2017)

The electronic stopping power of carbon for a swift C60 fullerene ion was calculated in a framework of dielectric function method as a function of speed ranging from 1 to 10 times the Bohr speed, where a C60 molecule is assumed to form a truncated icosahedron structure and the reduction of the cluster average charge is taken into account. Several cases of the expanded cages are also assumed. It is concluded that the cluster impacts do not reflect the equi-partition rule proved in the electronic energy loss of high energy point-charge projectiles and that swift C60 beams will provide an extremely dense energy-deposition implement.

Keywords; stopping power, C60, fullerene, average charge.

1. Introduction

In these two decades, progress in technology has made it possible to accelerate polyatomic projectiles or clusters at high energies [1], i.e., MeV to GeV for C60 fullerene and bio-molecules. This situation intensively stimulates our interest in investigating the interaction of high energy cluster ions with solid or biological materials both from the basic and applied viewpoints. Cluster impact has several advantages: reduction of the kinetic energy per atom at a given accelerated voltage, suppression of the charge-up effect in ion implantation, and performance of the high-density particle irradiation. In practice, these properties are utilized in fabrication and processes, e.g., surface evaporation and etching [2]. In basic research, on the other hand, the subjects using polyatomic ion beams are widely ranging, e.g., fragmentation [3-5], coulomb explosion [6,7].

Recent studies prove that a cluster projectile can bring new information that cannot be brought by a single particle ion. Here a significant role is performed with the number of constituent atoms and their spatial structure. In fact, they cause a strong correlation in time and space in collision phenomena. A typical term to characterize cluster impacts is 'sub-linear' or 'super-linear' dependence of a quantity of interest on the number of constituent atoms in a cluster. The sub-linear dependences have been found in the average charge per ion [8-10] and the secondary electron yield [11-14], while both the sub-linear and the super-linear dependences have been reported in the energy-loss phenomena [9, 15-19]. A recent study on the energy loss of MeV/atom linear-chained carbon clusters reveals the cooperative action between the average charge and the electronic excitation [20]. Here the sub-linear dependence of the cluster average charge is reconciled with the sub- and super-linear dependences of the energy loss over the energy range from 0.3 MeV/atom to 5 MeV/atom. This result

stresses that reduction of the average charge occurs in bulk. This sub-linear dependence was experimentally found [16,21]. The speed- dependence of the cluster average charge was reported for carbon clusters in ring and linear-chain structures [22]. Utilizing coulomb explosion technique, Chiba et al. [23] reported the quantitative reduction of the cluster average charge. As for a C60 projectile, Morita et al. [24] recently reported the cluster effect on the projected range under irradiation of 30 keV $C60^+$ and 0.5 keV C^+ ion.. In grazing scattering, energy loss of slow $C60^+$ ions [25] and multi-fragmentation of a C60 [26] were reported.

On the other hand, with progress of acceleration technology, swift fullerene projectiles has raised our interest in that we want to know to what extent the number of constituent atoms and its spatial structure influence the energy deposition in materials, and in that we want to investigate what kind of role a characteristic structure of a cage plays in electronic excitation. Under the above motivation, we presents the calculated result of the electronic stopping power of carbon for a C60 projectile with speed in a wide range from v_0 to $10\,v_0$. This reveals a new feature that has been found in neither atomic ions nor small cluster- ion irradiation. As a key quantity, we take into account reduction of the cluster average charge, which was already observed in small carbon clusters with MeV/atom energies [23]. In section 2, the framework of the present analysis is described, and in section 3, numerical results and discussion will be given. Through the paper, m, e and $\hbar$ denote, the electron rest mass, the elementary charge, and the Planck constant divided by 2π, respectively. The Bohr radius and the Bohr speed are denoted by $a_0 = \hbar^2/(me^2)$ and $v_0 = e^2/\hbar$, respectively.

2. Theoretical model

2-1. Atom position and pair-distribution function

It is known that a C60 molecule has an icosahedral symmetry [27]. An icosahedron has 20 faces of equilateral triangles, 12 vertices, and 30 edges. A C60 molecule is a truncated icosahedron, including 60 carbon atoms, 12 pentagons, 20 hexagons, and 30 double bonds. In the ground state structure, 60 atoms are on the surface of a sphere of radius $R_{cl} = 6.6\,a_0$. A schematic 3D view of atom positions are shown in fig. 1, where XYZ coordinate is in units of the Bohr radius. We assume here 60 isolated atoms are located on the positions of a truncated icosahedron and do not discern single- and double-bonds, because the average charge per ion of swift carbon clusters with speed higher than the Bohr speed tends to be greater than unity and consequently the outer-shell electrons are almost stripped off. Then we suppose that the molecular effect will play a negligible role. The spatial positions of 60 atoms are determined by considering symmetry on 5-fold axis. In our program, what we need to determine individual atom positions of a carbon-60 molecule is the input of a cluster radius. Once atom positions are determined, we can evaluate the spatial correlation of the pair-distribution function and the electronic stopping power, which depend on the relative distances of arbitrary two atoms.

The distribution of atoms in real space strongly influences the electron excitation as will be seen later. In order to grasp this effect, let consider the density correlation function $G(\vec{R})$ in real space for a cluster composed of n atoms located at $\vec{R}_j\,(j=1,\cdots,n)$, defined as

$$G(\vec{R}) = \sum_{j=1}^{n}\sum_{m=1}^{n}\delta(\vec{R}_j - \vec{R}_m + \vec{R}) \quad , \qquad (1)$$

using the distribution $\rho(\vec{r}) = \sum_{j=1}^{n}\delta(\vec{r} - \vec{R}_j)$ in real space. The Fourier transform of $G(\vec{R})$ is given by

$$G(\vec{k}) = n + n(n-1)g(\vec{k}) \quad , \qquad (2)$$

where $g(\vec{k})$ is the pair-correlation function in $\vec{k}$ space as

$$g(\vec{k}) = \frac{1}{n(n-1)} \sum_{j}^{n} \sum_{\ell(\neq j)}^{n} \exp\left\{ i\vec{k} \bullet (\vec{R}_j - \vec{R}_\ell) \right\} \quad . \qquad (3)$$

If we adopt statistical model, the structure factor of a C_{60} in the statistical model is given by

$$G_{st}(k) = n + n(n-1) \left[\frac{\sin(k R_{cl})}{k R_{cl}} \right]^2 . \qquad (4)$$

The variable $\vec{k}$ is connected with the momentum transfer vector to the excited quasi-particle in the individual or collective excitation modes, so that this function for a C60 plays a significant role in electron excitation. It is noted that $g(\vec{k})$ reflects the spatial structure of an incident cluster, but not reflect the charge states. Then the charge or average charges of individual partially stripped carbon ions also play an important role in cooperation with the structural information of $g(\vec{k})$.

2-2. Cluster average charge

It is well known that the average charge of a single ion moving in a material depends very weakly on the target material and it enables us to describe well only by the speed and the atomic number of the projectile ion. As for the cluster incidence, on the other hand, not only speeds of constituent ions but also spatial structure of the cluster and the number of atoms included in the cluster are important in practice. Here we consider briefly the average charge of a swift homo-atom cluster ion composed of N atoms with atomic number Z moving in a foil at speed v. According to the fluid-mechanical theory [9], the i-th constituent ion of the cluster will have the average charge Q_i, given by

$$\frac{Q_i}{Z} = \frac{2}{\sqrt{\pi}} \int_0^{y_i} dt \exp(-t^2) \quad , \quad y_i = \sqrt{\frac{3}{8}} \frac{\mathrm{v}}{\mathrm{v}_{b,i}}$$

$$\mathrm{v}_{b,i} = \left(1.092 Z^{4/3} + \sum_{j(\neq i)} 2\, V_{ji}(R_{ji}) \right)^{\frac{1}{2}} \mathrm{v}_0 . \qquad (5)$$

Here $V_{ji}(R_{ji})$ denotes the interaction potential energy per electron in atomic units of the i-th ion located at $\vec{R}_i$ with the j-th ion at $\vec{R}_j$. It is noted that the above equation reduces to the average charge of a single ion if the interaction potential term is dropped off. The interaction potential term represents the binding effect on the electron to be ionized, due to electron static forces of the surrounding ions. If $R_{ji}(=|\vec{R}_j - \vec{R}_i|)$ is large enough, $V_{ji}(R_{ji})$ reduces to the point-charge value Q_j / R_{ji}. As a more general expression, we take in the Thomas-Fermi-Moliere (TFM) approximation the following expression:

$$V_{ji}(R) = \frac{Q_j}{R} \left\{ 1 - \sum_{m=1}^{3} \alpha_m \exp\left(-\frac{\beta_m R}{\Lambda_i} \right) \right\} +$$

$$\frac{N_j}{R} \sum_{m=1}^{3} \sum_{\ell=1}^{3} \alpha_m \alpha_\ell \frac{\exp(-\beta_m R/\Lambda_i) - \exp(-\beta_\ell R/\Lambda_j)}{(\Lambda_i/\beta_m)^2 (\beta_\ell/\Lambda_j)^2 - 1}$$

with $\Lambda_t = 0.6269 N_t^{2/3} a_0 / (Z - N_t/7)$ and $N_t = Z - Q_t$ ($t = i, j$). Here, we have $\alpha_1 = 0.10$, $\alpha_2 = 0.55$, $\alpha_3 = 0.35$ and $\beta_1 = 6.0$, $\beta_2 = 1.20$, $\beta_3 = 0.30$.

By applying the present treatment, we evaluate the cluster average charge of a C60. This attracts our attention in the following aspects: first, there is no example to evaluate its average charge, and second, a C60 includes 60 atoms more than small carbon clusters include, and third, it has a hollow or fullerene structure. Later, we will show to what extent this characteristic cluster ion reduces its average charge, compared with that of a single ion with equivalent speed.

2-3. Electronic stopping force

Charged particles impinging on a dielectric medium induce the electric polarization through the dynamical dielectric function [28]. According to the dielectric function method, the expression of the electric stopping force acting on the incident cluster,

is given as

$$F_z = \frac{1}{2\pi^2 v}\int d\vec{k}\int_{-\infty}^{+\infty} d\omega \frac{-i\omega}{k^2}\left|\tilde{\rho}_c(\vec{k})\right|^2 \times\left[\frac{1}{\varepsilon(k,\omega)}-1\right]\delta(\omega-\vec{k}\bullet\vec{v}) \quad (6a)$$

with

$$\tilde{\rho}_c(\vec{k}) = e\sum_{j=1}^{n}\left[Z-\rho_{je}(\vec{k})\right]\exp(-i\vec{k}\bullet\vec{R}_j)\,. \quad (6b)$$

Here we assume that the incident cluster is regarded as an ensemble of isolated partially stripped ions with some bound electrons. In addition, it is assumed that the incident cluster has not any special orientations, in spite of a rigid spatial structure. Then we can take the orientation average over the angle between $\vec{k}$ and $\vec{R}_{j\ell}$, denoted by < >, as

$$\left\langle\left|\tilde{\rho}_c(\vec{k})\right|^2\right\rangle = e^2\sum_{j}^{n}\left[Z-\rho_{je}(k)\right]^2 + e^2\sum_{j}^{n}\sum_{\ell(\neq j)}^{n}\left[Z-\rho_{je}(k)\right]\left[Z-\rho_{\ell e}(k)\right]\frac{\sin(kR_{j\ell})}{kR_{j\ell}}\,. \quad (7)$$

Then the electronic stopping power S of a material, which is the magnitude of this friction force, reads

$$S = \frac{2}{\pi v^2}\int_0^{+\infty} dk\,\frac{1}{k}\left\langle\left|\tilde{\rho}_c(\vec{k})\right|^2\right\rangle\int_0^{kv} d\omega\,\omega\,\Im m\left\{\frac{-1}{\varepsilon(k,\omega)}\right\}\,. \quad (8)$$

Here we utilize that the real part and the imaginary part of $\varepsilon(\vec{k},\omega)$ is, respectively, even-function and odd-function of ω. Here we have to take into account the average charge reduction in estimating the square average of the cluster charge density in Fourier space in a self-consistent manner. If we neglect the average charge reduction, namely, adopt the assumption that the average charge of individual ions in the cluster are all equal to $\rho_j(k)=\rho(k)\,(j=1,2,\cdots,60)$, then we see the eq.(7) reduces to

$$\left\langle\left|\tilde{\rho}_c(\vec{k})\right|^2\right\rangle = \left[\rho(k)\right]^2 G(k)\,, \quad (9)$$

$$G(k) = n+\sum_{j}^{n}\sum_{\ell(\neq j)}^{n}\frac{\sin(k\,R_{j\ell})}{k\,R_{j\ell}}\,. \quad (10)$$

Here $G(k)$ is the structure factor, determined by the initial structure of the icosahedron. Thus, approximately speaking, the square of the external charge density is described by the structure factor multiplied by the square charge density. The former reflects the spatial structure of the incident cluster.

2-4. Satisfaction of the sum rule

It is well known that the dielectric function of an electron gas represents two excitation modes. One is the single electron excitation mode and the other is the plasmon (or, collective) excitation mode. The analytical expression for the electron gas at absolute zero temperature was obtained [28]. Now we assume that four outer-shell electrons per carbon atom participate in the electron gas. This assumption leads to a bulk plasmon energy $\hbar\omega_p = 25\,\mathrm{eV}$ for carbon target. According to the optical measurement, on the other hand, the excitation spectrum of a plasmon is slightly broad, and this reflects a finite lifetime of a plasmon. In order to take into account this fact, we adopt the expression of the inverse dielectric function as

$$\frac{1}{\varepsilon(k,\omega)} = 1+\frac{{\omega_p}^2}{\omega^2-\omega_p(k)^2+i\omega\gamma}\,, \quad (11)$$

where the damping constant γ, relating to the lifetime of a plasmon, is set to $\hbar\gamma = 3.3\,\mathrm{eV}$. In addition, the dispersion of a plasmon is introduced as follows:

$$\omega_p(k)^2 = {\omega_p}^2+\frac{3}{5}{v_F}^2k^2+\left(\frac{\hbar}{2m}\right)^2 k^4\,, \quad (12)$$

with the dispersion-less plasma frequency $\omega_p = \left(4\pi n e^2/m\right)^{1/2}$. A plasmon is well defined in the region of $k \le k_{cut}$. Here k_{cut} is the cut-off wave number, beyond which the plasmon excitation

branch is buried into the individual electron excitation branch. In general, regardless of the wave number, the inverse dielectric function has to satisfy the sum rule as

$$\int_0^{+\infty} d\omega\, \omega\, \Im m\left(\frac{-1}{\varepsilon(k,\omega)}\right) = \frac{\pi}{2}\omega_p{}^2 \quad . \qquad (13)$$

At small k, the contribution of the plasmon excitation branch is proved to be dominant to the sum rule. In practice, following a mathematical formula, one can prove that eqs.(12) and (13) lead

$$\int_0^{+\infty} d\omega \frac{\omega_p{}^2\omega^2\gamma}{\left[\omega^2-\omega_p(k)^2\right]^2+(\omega\gamma)^2} = \frac{\pi}{2}\omega_p{}^2 . \qquad (14)$$

On the other hand, at relatively high k, we confirmed by numerical estimation that the individual electron excitation branch holds the sum rule within a high accuracy. Then we intend to fulfill the sum rule regardless of the wave number, by introducing a k-dependent factor $F(k)$, which means the fraction of the contribution of the plasmon excitation, such that $F(k)=1$ for $k<k_1$ and $F(k)=0$ at $k=k_{cut}$. For $k_1<k<k_{cut}$, $F(k)$ is set to be the 8^{th} polynomials of $F(k)=\sum_{m=0}^{8} A_m k^m$, where the coefficients $A_m (m=0-8)$ are determined together with the value of k_1 and k_{cut} so as to fulfill the sum rule with an accuracy of 5 percent error. As a summary of this part, the function $F(k)$ denoted the contribution of the damped plasmon excitation. In addition to the excitation of the conduction electron, the excitation of two inner-shell electrons is taken into account in the dielectric formalism [29].

3. Numerical Results and Discussion.

Figure 2 shows the structure factors, where the thick solid line indicates $G(k)$ in eq.(2), which is calculated using the atom positions, and the thin solid line shows $G_{st}(k)$ in eq.(4). In a small-k region, both structure factors yield almost the same value, and around up to $k=2$ (atomic unit), both have similar oscillatory structures. Beyond $k=4$ (atomic unit), $G_{st}(k)$ tends to be constant with vanishing oscillation. On the other hand, the oscillatory structure of $G(k)$ does not disappear over a wide range of k indicated, and the amplitude of oscillation is larger than that of $G_{st}(k)$. It is noted that the value of the structure factor at $k=0$, i.e., $G(0)$ or $G_{st}(0)$, yields the square of the total number of atoms in a cluster.

Figure 3 shows the average charge per ion $Q(60)$ of a C60 cluster and $Q(1)$ of a single carbon ion, calculated as a function of speed in units of the Bohr speed. The thin solid line refers to a single carbon ion, for reference. The dot-dot-dash line, the dot-dash line, and the dash line refer to a C60 with radius of $R_{cl}=6.6\,a_0$, $8\,a_0$, and $10\,a_0$, respectively. Here, in order to show to what extent the cluster expansion influences, we prepare two expanded cases, $R_{cl}=8\,a_0$ and $R_{cl}=10\,a_0$ together with the initial case of $R_{cl}=6.6\,a_0$. There are several important remarks in this figure. First, compared with a single carbon ion, the average charge per ion of a C60 with cluster radius of $R_{cl}=6.6\,a_0$ reduces to about 60 percent in the velocity range of $2<v/v_0<7$. This reduction of the cluster average charge is much larger than those of small linear-chain clusters. For example, the average charge ratio for a C10 is more than 70 percent at 2 MeV/atom [22]. The reason of this aspect is that the number of the neighboring atoms surrounding a given atom is more so that the binding

effect becomes stronger on the electrons to be ionized. Second, the cluster expansion from $R_{cl} = 6.6\,a_0$ to $R_{cl} = 10\,a_0$ does not increase the average charge so much. The increase in the average charge amounts to at most 10 percent over the speed range studied. Of course, an extreme expansion of the cluster that individual ions are little affected from other ions, leads the cluster average charge to the corresponding value of a single ion at the equivalent speed. Third, it should be noted that the average charges of individual component atoms result in the same value, since each atom position is symmetrically equivalent in this theoretical model.

Next, before presenting the stopping for a C60, we briefly describe the background on the electronic stopping power of materials for a single ion. In general, the stopping power curve for a single ion, whether it is a point charge or a partially stripped ion (PSI), presents a single peak profile. For a swift point charge projectile, Lindhart proved the equi-partition rule that the contribution of the individual electron excitation is equal to that of the collective (plasmon) excitation [28]. On the other hand, for a PSI, the contribution of the individual electron excitation is larger than that of the collective one. This fact is understood by the following reason: for the collective excitation the net charge of a PSI works dominantly in practice because this excitation is induced in distant collision, while for the individual electron excitation induced in close collision the electric charge of a PSI effectively works larger than the net charge where the bound electrons can screen the projectile's nuclear charge only partially [30].

Figure 4 represents the electronic stopping cross section of the conduction electrons in carbon for a C60 cluster, where the solid line, the dashed line and the dot-dash line indicate the cases of $R_{cl} = 6.6\,a_0$, $8\,a_0$, and $10\,a_0$, respectively. Here we give a special remark that the electric stopping is distinctly composed of two peaks. One is the peak locating around at $v = 2v_0$ and another is a 'giant resonance' peak appearing in a wide speed range of $v > 4v_0$. The former peak weakly depends on the cluster radius, while the 'giant resonance' peak strongly depends on the cluster radius. In order to elucidate this structure in the stopping power, we show, as an example for a C60 with $R_{cl} = 6.6\,a_0$, the contribution of the single-electron excitation by the dot-dot-dash line, and that of the collective excitation by the thin dash line. Then we understand the giant resonance originates from the collective excitation. Why does the plasmon excitation contribute so much? The reason is as follows: The plasmon excitation is induced in distant collision so that small momentum transfer ($\hbar k$) from a projectile to an electron gas plays a significant role. The wave length $\lambda \simeq 13\,a_0$ $(= 2R_{cl})$ of a plasmon corresponds to its wave number $k = 2\pi / \lambda = 0.5(a.u.)$. Then a plasmon with wave length $\lambda > 2R_{cl}$ (or, $k < 0.5(a.u.)$) tends to see a C60 projectile as an unified-ion projectile having 60 ions. In this case, most of constituent ions in a C60 will coherently participate in plasmon excitation. This fact can be realized the value of the structure factor in fig.2 yields $G(k) \simeq 3600$ at very small k value. The value of the structure factor increases extremely with decreasing momentum transfer. In addition, as the cluster speed increases, the dominant momentum transfer range contributing to plasmon excitation becomes wider. Namely, the plasmon excitation is allowed for $k_{\min} < k < k_{\mathrm{cut}}$ at a given ω, where $k_{\min} \equiv \omega / v$ and k_{cut} is the cut-off wave number [31]. Moreover, the net charge in Fourier space, i.e., $\rho_j(\vec{k})$ in eq.(7) or $\rho(k)$ in eq.(9), increases as the incident speed increases. Thus, appearance of the giant resonance structure is the result of cooperation of the spatial structure and

the average charge. If the structure factor is set to unity, one obtains the stopping cross section for the single carbon incidence.

Next, we have interest in the size dependence of the giant resonance. Figure 4 represents the dependence of the electronic stopping cross section of carbon for a C60 projectile on its radius R_{cl}. The solid line, the dashed line, and the dot-dash line represent the result for $R_{cl} = 6.6\,a_0$, $8\,a_0$, and $10\,a_0$, respectively. As far as the cluster speed is less than $2.5\,v_0$, the calculated stopping cross section for a C60 depends very weakly on R_{cl}. On the other hand, once the cluster speed exceeds $2.5\,v_0$, the stopping cross section for a C60 decreases largely with increasing R_{cl}, in spite of keeping a giant resonance character. This is due to the behavior of the structure factor. For example, the first dip, located at $k \approx \pi / R_{cl}$ in the structure factor in fig.1, shifts toward the smaller-k side for a larger R_{cl}. This means that the structure factor contributing to the plasmon excitation is suppressed and as a result the plasmon contribution becomes smaller. At lower speed, i.e., $v < 2.5\,v_0$, the main contribution to the stopping is the individual electron excitation, which requires relatively large momentum transfer, or, close collision, so the main peak in the structure factor does not play a significant role.

In order to see the dependence of the stopping cross section per atom on the cluster radius R_{cl}, we show in fig.5 the ratio R_{st} of the stopping power per atom of carbon for a C60, $S(60)$, with $R_{cl} = 6.6 - 10\,a_0$ to that for a single carbon ion, $S(1)$. The solid line, the dashed line, and the dot-dash line refer to $R_{st} = S(60)/[60 \times S(1)]$ for a C60 with $R_{cl} = 6.6\,a_0$, $8\,a_0$, and $10\,a_0$, respectively. One can see that R_{st} is less than unity in the speed range of $\mathrm{v} < 4\,\mathrm{v}_0$ for the cluster with $R_{cl} = 6.6\,a_0$. This is called the sub-linear cluster effect in the electronic stopping. Once the cluster speed exceeds the above range, the ratio R_{st} grows rapidly with increasing speed, and the super-linear cluster effect appears. The threshold speed v_{th}, at which we define $R_{st} = 1$ and the sub-linear (super-linear) effect appears in the range of $\mathrm{v} < \mathrm{v}_{th}$ ($\mathrm{v} > \mathrm{v}_{th}$), becomes larger as the C60 expands uniformly. The main reason of the sub-linear cluster effect is the reduction of the cluster average charge, shown in figure 2. On the other hand, the super-linear cluster effect originates from the strong spatial correlation of atoms in the structure factor. The reduction of the cluster average charge incorporated practically always works toward the sub-linear effect. Nevertheless, the correlation appearing in the structure factor surpasses the average charge reduction contribution and results in leading to the super-linear cluster effect.

In conclusion, we theoretically studied the electronic stopping power of carbon for a C60 fullerene cluster ion with use of the dielectric-function formalism. The spatial structure is assumed to form a truncated icosahedron and the reduction of the cluster average charge was taken into account. Regarding the average charge, the sub-linear effect is newly predicted for a C_{60}, regardless of the incident speed. This sub-linear effect is found to be much more enhanced than that previously proposed for the linear-chained small carbon clusters [22]. In the electronic stopping of carbon, apart from the normal peak profile nearly located at speed of 2 times the Bohr speed, we found a giant resonance profile due to the plasmon

excitation, which appears at higher speeds over a wide range of speeds greater than 4 times the Bohr speed, and extremely surpasses the individual excitation contribution. This feature violates the equi-partition rule proved in the electronic stopping power for swift point charges. The giant resonance is very unique to swift large cluster projectiles, especially with cage structure. This result will open a new door of energy deposition by swift cluster ions, which can be attained neither by small cluster ions nor by a single atomic ion, even if it would have a hundred times elementary charge. I would like to expect progress in acceleration of swift fullerene ions.

References

[1] P. Attal, S. Della-Negra, D. Gardes, J.D. Larson, Y. Le. Beyec, R. Vienet-Legue, and B. Waast, Nucl. Instr. Meth. in Phys. Res. A 328, 293 (1993).

[2] I. Yamada, J. Matsuo, N. Toyoda, and A. Kirkpatrick, Materials Science and Engineering R34, 231 (2001).

[3] B. Farizon M. Farizon, M.J. Gaillard, E. Gerlic, and S. Ouaskit, Nucl. Instr. Meth. in Phys. Res. B 88, 86 (1994).

[4] A. Itoh, H. Tsuchida, T. Majima and N. Imanishi, Phys.Rev. A 59, 4428 (1999); A. Itoh, H. Tsuchida, T. Majima, S. Anada, A. Yogo and N. Imanishi, Phys. Rev. A 61, 012702 (1999) ; H. Tsuchida, A. Itoh, K. Miyabe, Y. Bitoh and N. Imanishi, J. Phys. B 32, 5289 (1999).

[5] T. LeBrun, H.G. Berry, S. Cheng, R.W. Dunfort, H. Esbensen, D.S. Gemmell, E.P. Kanter, and W. Bauer, Phys. Rev. Lett. 72, 3965 (1994).

[6] A. Faibis, G. Goldring, M. Hass, R. Kaim, I. Plesser and Z. Vager, Nucl. Instr. Meth. 194, 299 (1982).

[7] A. Chiba, Y. Saitoh, K. Narumi, Y. Takahashi, K. Yamada and T. Kaneko, Nucl. Instr. Meth. in Phys. Res. B 269, 824 (2011).

[8] A. Brunelle, S. Della-Negra, J. Depauw, D. Jacquet, Y. LeBeyec, M. Pautrat, Phys. Rev. A 59, 4456 (1999).

[9] T. Kaneko, Phys.Rev. A 66, 052901 (2002).

[10] A. Chiba, Y.Saitoh, K. Narumi, M. Adachi, and T. Kaneko, Phys. Rev. A 76, 063201 (2007).

[11] H. Kudo, W. Iwazaki, R. Uchiyama, S. Tomita, K. Shima, K. Sasa, S. Ishii, K. Narumi, H. Naramoto, Y. Saitoh, S. Yamamoto and T. Kaneko, Jap. J. Appl. Phys. 45, *L565* (2006).

[12] S. Tomita, S. Yoda, R. Uchiyama, S. Ishii, K. Sasa, T. Kaneko and H. Kudo, Phys. Rev. A 73, 060901(R) (2006).

[13] T. Kaneko, H. Kudo, S. Tomita, and R. Uchiyama, J. Phys. Soc. Jpn. 75, 034717 (2006).

[14] H. Kudo, H. Arai, S. Tomita, S. Ishii and T. Kaneko, Vacuum 84, 1014 (2010).

[15] M. Vicanek, I. Abril, N.R. Arista, and A. Gras-Marti, Phys. Rev. A 46, 5745 (1992)

[16] A. Brunelle, S. Della-Negra, J. Depauw, D. Jacquet, Y. Le. Beyec, M. Pautrat, and Ch. Schoppmann, Nucl. Instr. Meth. in Phys. Res. B 125, 207(1997).

[17] T. Kaneko, Nucl. Instr. Meth. in Phys. Res. B 153, 15 (1999).

[18] E. Ray, R. Kirsch, H.H. Mikkelsen, J.C. Poizat, and J. Remillieux, Nucl. Instr. Meth. in Phys. Res. B69, 133 (1992).

[19] K. Baudin, A. Brunelle, M. Chabot, S. Della-Negr, J. Depauw, D. Gardes, P. Hakansson, Y. Le. Beyec, A. Billebaud, M. Fallavier, J. Remillieux, J. C. Poizat, and J.P. Thomas, Nucl. Instr. Meth. in Phys. Res. B 94, 341(1994).

[20] Toshiaki Kaneko, Phys. Rev. A 86, 012901 (2012).

[21] S. Tomita, M. Murakami, N. Sakamoto, S. Ishii, K. Sasa, T. Kaneko, and H. Kudo, Phys. Rev. A 82, 044901 (2010).

[22] T. Kaneko, K. Ihara, and M. Kohno, Nucl. Instr. Meth. in Phys. Res. B 315(2013) 76-80.

[23] A. Chiba, Y. Saitoh, K. Narumi, K. Yamada, T. Kaneko, Nucl.Instr.Meth. in Phys. Res. B 315(2013) 81-84.

[24] Y. Morita, K. Nakajima, M. Suzuki, K. Narumi, Y. Saitoh, W. Vandervorst, and K. Kimura, Nucl. Instr. Meth. In Phys. Res. B269, 2080 (2011).

[25] T. Matsushita, K. Nakajima, M. Suzuki, and K. Kimura, Phys. Rev. A 76, 032903 (2007).

[26] A. Kaplan, A. Bekkerman, B. Tsipinyuk, and E. Kolodney, Phys. Rev. B 82, 245421 (2010).

[27] Djuro Koruga, Stuart Hameroff, James Withers, Raoulf Loutfy, Malur Sundareshan, 'Fullerene C60' (Horth-Holland, 1993)

[28] J. Lindhard and A. Winther, K. Dan. Vidensk. Selsk. Mat. Fys. Medd. 34(4) (1964) 1.

[29] T. Kaneko, Phys. Rev. A40, 2188 (1989) ; Phys. Stat. Sol. B156, 49 (1989) ; Atom. Dat. Nucl. Dat. Tab. 53, 271 (1993).¥

[30] T. Kaneko, Phys. Rev. A33, 1602 (1986) ; Phys. Rev. A49, 2681(1994) ; Phys. Rev. A51, 535(1995).

[31] D. Pines, 'Elementary excitations in solids' (Benjamin Press, 1964).

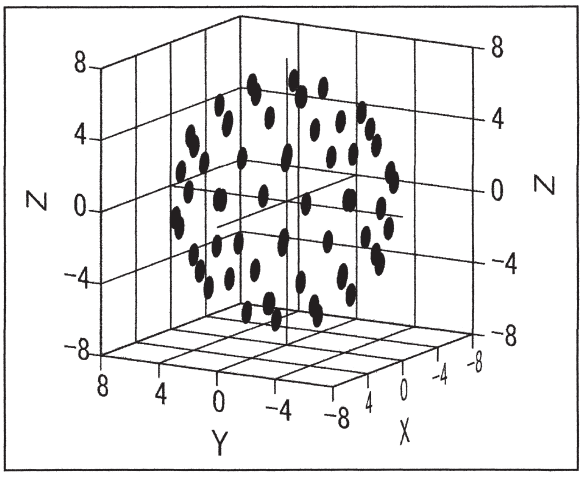

Fig.1: A schematic 3D view of atom positions in a C60 cluster on a sphere of radius $R_{cl} = 6.6\,a_0$ in units of the Bohr radius a_0.

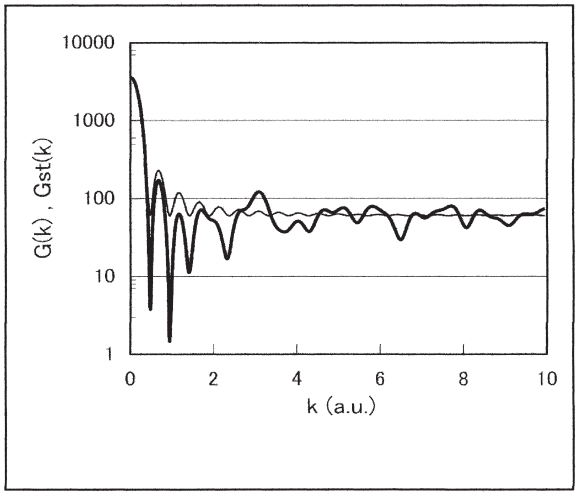

Fig. 2: Structure factor of a C60 cluster with radius of $R_{cl} = 6.6\,a_0$ as a function of k in atomic units (in units of $1/a_0$). The solid line indicates $G(k)$ and the dashed line shows $G_{st}(k)$.

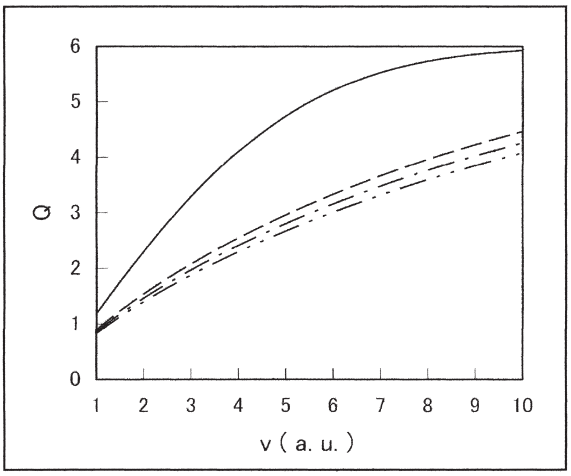

Fig. 3: Average charge per ion of a C60 cluster with radius of $R_{cl} = 6.6\,a_0$ (dot-dot-dash line), $R_{cl} = 8\,a_0$ (dot-dash line), and $R_{cl} = 10\,a_0$ (dash line), together with that of a single carbon ion (thin solid line), as a function of speed v in atomic units (in units of v_0).

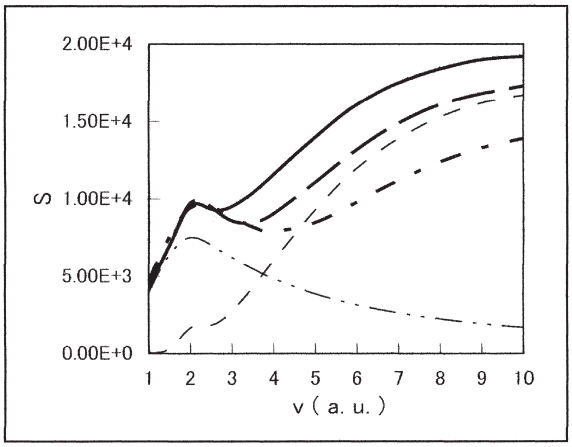

Fig. 4 : Calculated stopping cross section S of carbon for a C60 fullerene in units of $eVcm^2/10^{15}$atoms as a function of speed v in units of v_0. The solid line, the dashed line, and the dot-dash line show the total value for a C60 fullerene with radius of $R_{cl} = 6.6\,a_0$, $R_{cl} = 8\,a_0$, and $R_{cl} = 10\,a_0$. The thin dash line and the dot-dot-dash line indicate the contributions of the plasmon and the single-electron excitation for a C_{60} with $R_{cl} = 6.6\,a_0$.

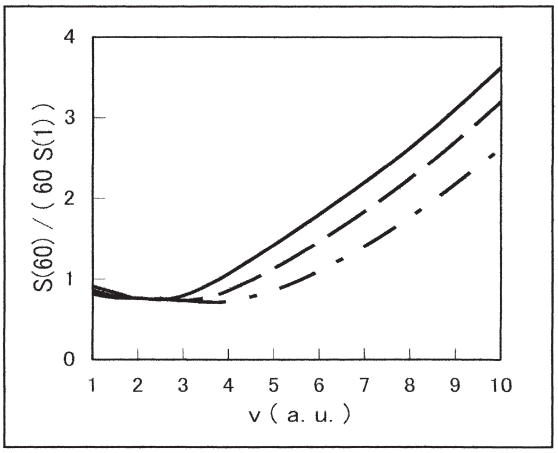

Fig. 5: Ratio of the stopping cross section per atom, $S(60)/(60\times S(1))$, with radius of $R_{cl}=6.6\,a_0$ (solid line), $R_{cl}=8\,a_0$ (dashed line), and $R_{cl}=10\,a_0$ (dot-dash line) as a function of speed v in units of v_0.